Journal of Hazardous Materials, 33 (1993) 307–318
Elsevier Science Publishers B.V., Amsterdam

Expansion zone modeling of two-phase and gas discharges

John L. Woodward

DNV Technica Inc., 355 East Campus View Boulevard, Columbus, OH 43235 (USA)

Abstract

An expansion zone model couples a discharge rate model with a high momentum jet dispersion model for sonic or choked flow. Conventional expansion zone modeling, as based on an overall force balance, predicts large increases in the expansion zone diameter and only moderate increases in the expansion zone velocity at a range of low superheat. Alternately, it is shown that any analytic solution for a discharge model can be used also as an expansion zone model. In particular, the homogeneous equilibrium model (HEM) for two-phase discharge and the model for isentropic discharge of an ideal gas are used to exemplify expansion zone modeling. The new approach predicts, in contrast to the conventional approach, large increases in velocity and only moderate increases in expansion zone diameter. Experimental data are needed to decide which model is more nearly correct.

1. Introduction

An expansion zone model couples the predictions of a discharge rate model and a jet dispersion model as depicted in Fig. 1. Accidental leaks from a vessel or pipe often occur from a noncircular source such as a loose flange; but are usually modeled as a discharge from a round orifice or pipe of equivalent discharge area. Such a discharge develops a converging zone and an expansion zone.

Discharge modeling concentrates on the converging zone, since the mass discharge rate is determined by the mass flux at the choke point, G_2, and the discharge coefficient, C_D, in addition to the discharge area, A_1. Air entrainment is usually assumed negligible in both the converging and expansion zones and is treated by the jet dispersion model. The inputs needed by the jet dispersion model are provided by the expansion zone model. These include the velocities of the vapor and liquid, jet diameter, vapor quality, temperature, and density or mass discharge rate. The velocity is important in establishing the mean drop size by the mechanism of aerodynamic breakup.

Correspondence to: John L. Woodward DNV Technica Inc., 355 East Campus View Boulevard, Columbus, OH 43235 (USA) Fax: (614) 848-3955.

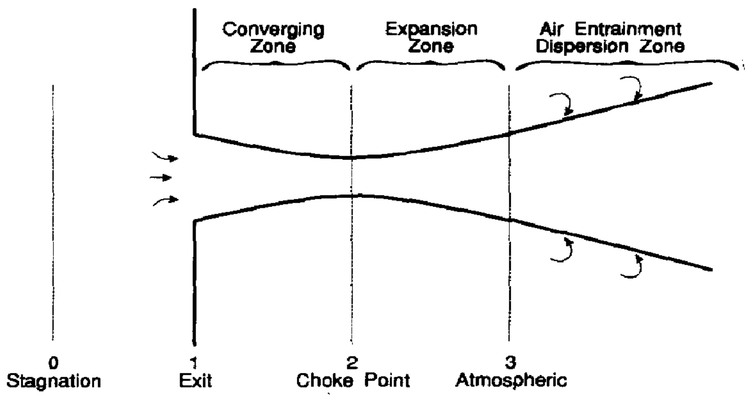

Fig. 1. Definition of terms for high-momentum jet discharge from an orifice.

Moodie and Ewan [1] explored the expansion zone and provided a model for gas jets and some data for two-phase jets. Their gas jet model made use of an empirical centerline momentum model attributed to Kleinstein [2]. An empirical approach was advocated to account for the temperature change across the shock wave which develops at the choke point as flow becomes sonic.

In practice, the expansion zone model predictions are an integral part of subsequent dispersion modeling which are tuned to match available experimental data. Thus, whenever changes are made to the expansion zone model, the dispersion model must be retuned to fit the data. The approach recommended here assumes negligible temperature change across the shock wave. The validity of this assumption is considered hereafter, but, in any event, a change in this assumption would likely be "washed out" by subsequent retuning of the dispersion model.

2. Converging, expanding flow

As illustrated in Fig. 1, contraction occurs as the fluid accelerates upon leaving an orifice or entering a nozzle as pressure drops from the stagnation pressure, P_0, to the choked pressure, P_2. The area at the choke point, A_2, is given by

$$A_2 = C_D A_1 \tag{1}$$

where A_1 is the discharge area and C_D is the discharge coefficient have a value typically in the range

$$0.5 < C_D < 1.0$$

Bragg [3] showed that C_D can be calculated considering the acceleration from P_0 to P_1 once P_2 is known. For subcooled liquids, $C_D = 0.61$, but for saturated liquids and gases, $C_D \rightarrow 1.0$ using Bragg's formulas.

As the pressure in the discharging jet further decreases from P_2 to P_3, where P_3 is usually the atmospheric pressure, P_a, the jet expands. Churchill [4] points out that for compressible flow contraction is characteristic of accelerating subsonic flow (Mach Number <1) and expansion is characteristic of accelerating supersonic flow (Mach Number >1). In addition, flashing liquids expand because the flashing decreases the two-phase density. Two-phase density is very sensitive to the vapor quality, x, in the range $0<x<0.01$.

3. Conventional model based on force balance

A commonly cited expansion zone model, used for example by Fauske and Epstein [5] is attributed to Dryden et al. [6]. This model is derived from an overall force balance, including the annular area A_3-A_1 as follows.

$$wu_1 - wu_3 + P_1 A_1 + P_3(A_3 - A_1) - P_3 A_3 = 0$$

which, since

$$w = G_1 A_1 = G_3 A_3 \tag{2}$$

reduces to

$$u_3 = u_1 + \frac{P_1 - P_3}{G_1} \tag{3}$$

where

$$G_1 = C_D G_2$$

The expansion zone area is

$$A_3 = \frac{wv_3}{u_3} \tag{4}$$

where v_3 is given by eq. (12).

4. Expansion zone model for ideal gas discharge

The well-known solution for the discharge of an ideal gas can be used to illustrate how to obtain an alternative expansion zone model. For isentropic expansion of an ideal gas the specific volume and temperature at the end of the expansion zone are given by [7]

$$\frac{v_0}{v_3} = \left(\frac{T_3}{T_0}\right)^{1/(k-1)} = \eta_a^{1/k} \tag{5}$$

With this equation of state, the momentum balance is integrated in standard texts (for example Churchill [8]) to give

$$G^{*2}=\left(\frac{2k}{k-1}\right)\eta^{2/k}(1-\eta^{(k-1)/k}) \tag{6}$$

where η is the dimensionless pressure ratio and G^* is the dimensionless mass flux. Equation (6) applies for subsonic flow when $\eta=\eta_a>\eta_c$ where

$$\eta_c=\left[\frac{2}{k+1}\right]^{k/(k-1)} \tag{7}$$

and for $\eta=\eta_a<\eta_c$, the flow is choked (sonic) and

$$G_c^*=k\left[\frac{2}{k+1}\right]^{(k+1)/(k-1)} \tag{8}$$

Figure 2 plots eqs. (6) and (8) using the following dimensionless variables

$$\rho^*=\frac{1}{2}\left(\frac{\rho}{\rho_c}\right)=\frac{1}{2}\left(\frac{\eta}{\eta_c}\right)^{1/k} \tag{9a}$$

$$u^*=\frac{1}{2}\left(\frac{u}{u_c}\right)=\frac{1}{2}\frac{G^*}{G_c^*(\rho/\rho_c)}=\frac{1}{2}\frac{G^*}{G_c^*}\left(\frac{\eta_c}{\eta}\right)^{1/k} \tag{9b}$$

$$A_3=A_2\frac{G_c^*}{G^*(\eta)} \tag{9c}$$

The parameter value of $k=1.2$ is used in Fig. 2 for which $\eta_c=0.5645$. We use $A_2=0.75$ in Fig. 2 simply for clarity of plotting. Figure 2 shows G^*, u^* and A at

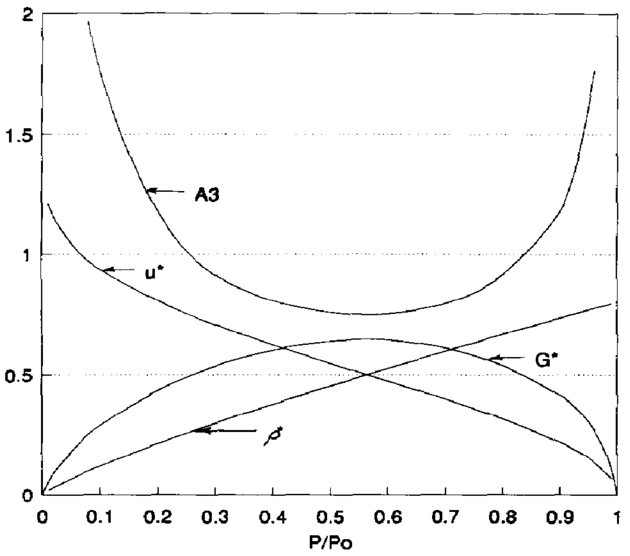

Fig. 2. Adiabatic gas discharge profiles ($k=1.2$).

any value of $\eta = P/P_0$. In particular, at $\eta_c = P_c/P_0$, the choked conditions are reached and A is at a minimum value, A_2.

At values of $\eta_a = P_a/P_0$, the expansion zone conditions are reached, assuming only that the solutions given by eq. (9) apply across a shock wave which could develop at the throat. Figure 2 shows the expansion zone area increasing as the mirror image to the decreasing G^* function. The expansion zone velocity, expressed as $u^*(\eta_a)$ increases by as much as a factor of two over the velocity at the choke point if η_a is as low as 0.06.

5. Expansion zone modeling for two-phase discharge

The approach just illustrated is a general one, and can be readily applied to any analytic solution for the discharge of a compressible fluid. A number of such solutions have been developed and expressed as $G^*(\eta)$, each with the characteristic that the $G^*(\eta)$ function is zero at the extremes $\eta = 0$ and 1, and so reaches a maximum at an intermediate point η_c giving the choked flux $G_c^*(\eta_c)$. Any such solution can be evaluated at $\eta = \eta_a$ to give $G_{amb}(\eta_a) = G_3$ which, by the definition $G_3 = u_3/v_3$ gives the expansion zone velocity

$$u_3 = v_3 G_3(\eta_a) = G^*(\eta_a)(P_0 \rho_0)^{-1/2} v_3 \tag{11}$$

where

$$v_3 = [x v_G + (1-x) v_L]_3 \tag{12}$$

Mass continuity gives the expansion zone area, A_3

$$w = C_D A_1 G_C = A_3 G_{amb}$$

or

$$A_3 = C_D A_1 \frac{G_C^*(\eta_C)}{G_3^*(\eta_a)} = \frac{\pi}{4} D_3^2 \tag{13}$$

For equilibrium models of flashing liquids, vapor quality is given by an isentropic flash, assuming vapor–liquid equilibrium

$$x_3 = \frac{S_{LO} - S_{L3}}{S_{GL}} \tag{14}$$

However, it is well established that equilibrium is not established for orifice discharge, or for short nozzles or pipes (Henry [9], Morris [10], Hardekopf and Mewes [11], and Fauske [12]). For this reason, it is more appropriate to apply a nonequilibrium model, such as that suggested by Henry and Fauske [13]. They postulate that the nonequilibrium vapor quality is related to the equilibrium vapor quality by

$$x_3 = N x_{e3}$$

where Fauske in [DIERS, 14] recommends

$$N=\begin{cases} x_{e3}/0.14 & x_{e3}\le 0.14 \\ 1.0 & x_{e3}>0.14 \end{cases}$$

as an empirical correlation which matches predictions to observed data.

The temperature in this case is the liquid saturation temperature, $T_S(P_a)$. If $\eta_s<\eta_a$, $x_3=0$, and there is no expansion in the expansion zone. If this case $G^*_{amb}=G^*_C$ and eq. (13) reduces to

$$A_3=A_2=C_D A_1 \tag{15}$$

for highly subcooled, nonflashing liquid flow.

5.1 Application with HEM

As an example, the above solutions are illustrated for the homogeneous equilibrium model (HEM) for flashing and subcooled liquid flow by Leung [14] and Leung and Grolmes [15].

The HEM assumes nonslip flow, $u_G=u_L$, and thermodynamic equilibrium along the flow path. Other assumptions are $x=x_0=$constant (frozen flow), isothermal flow, $v_G\gg v_L$, $H_{LG}=H_{LGO}$, $C_{PL}=C_{PLO}$, and that v_{GLO} can replace $v_{GL}(P)$. In spite of these quite restrictive assumptions, the HEM has gained wide acceptance as an adequate approximation, for example by AIChE's DIERS (Design Institute of Emergency Relief Systems) [16–18]. It is known to provide a lower bounding approximation [19] for orifice (nonequilibrium) flow, and an adequate model for nozzle or pipe (equilibrium) flow.

The HEM integrates the pressure derivative of eq. (12) from P_0 to P to define a correlating parameter ω given by

$$\omega=\frac{x_0 v_{GO}}{v_0}+\frac{T_0 P_0 C_{PLO}}{v_0}\left[\frac{v_{GLO}}{H_{GLO}}\right]^2 \tag{16}$$

The first term is α_0 the initial void fraction. The two-phase specific volume is related to ω by

$$\frac{v}{v_0}=\frac{\omega}{\eta}+(1-\omega)$$

For frictionless nozzle or orifice flow, the momentum balance is integrated to give

$$G^*=\frac{\left[2\left((1-\eta_s)+\omega\eta_s\ln\frac{\eta_s}{\eta}+(1-\omega)(\eta_s-\eta)\right)\right]^{1/2}}{\omega\frac{\eta_s}{\eta}+(1-\omega)} \tag{17}$$

The critical mass flux is found by setting $dG^*/d\eta=0$ to give the following transcendental equation which gives the critical pressure ratio, η_C implicitly

$$\frac{(\omega-1)^2}{2\omega\eta_S}\eta^2-2(\omega-1)\eta+\left(\frac{3}{2}\omega\eta_S-1\right)-\omega\eta_S\ln\frac{\eta_S}{\eta}=0 \tag{18}$$

Once η_C is found as a root of eq. (18), G_C^* is given by

$$G_C^* = \eta_C / \omega^{1/2} \tag{19}$$

Equation (18) applies when flashing occurs before or at the choke point. If flashing occurs after the choke point, it affects the expansion zone, but not the discharge rate. In this case the discharge rate is given by the liquid-phase Bernoulli equation. Leung [15] found that a criterion for determining whether flashing occurs before or after the choke point is

If

$$\eta_S < \frac{2\omega_s}{1+2\omega_s} \tag{20}$$

then flashing occurs in the expansion zone, and mass flux is given by the Bernoulli equation

$$G_C^* = [2(1-\eta_C)]^{1/2} \tag{21a}$$

with

$$\eta_C = \max(\eta_S, \eta_a) \tag{21b}$$

Otherwise, η_C is given by eq. (18) and G_C^* by eq. (19).

6. Comparison of models

Typical predictions of the alternative models are given for a flashing liquid in Figs. 3–5 for the new model (eqs. 11–15, with the HEM, eqs. 17–21) and in Fig. 6 for the conventional model (eqs. 3 and 4). These depict constant pressure discharge of propane from 8 atm tank pressure with one meter of liquid head through a 50 mm orifice. For subcooled tank temperatures ($T < 231$ K) the expansion zone area in either case is given by eq. (15). The models differ most for temperatures just above the normal boiling point. In this region, the conventional model predicts a large increase in diameter and, consequently, a mild increase in velocity. In contrast, the new model predicts a moderate increase in diameter, since the ratio G_2/G_3 is near unity in the low subcooled region. Correspondingly, the new model predicts a large increase in velocity.

This behavior occurs because the two-phase density drops rapidly with slight increases in vapor quality as shown in Fig. 4. For the conventional model A_3 is linear in specific volume, v_3, whereas for the new model, u_3 is linear in v_3. Thus, using the nonequilibrium vapor quality reduces the predicted A_3 in Fig. 6 and the predicted u_3 in Fig. 3.

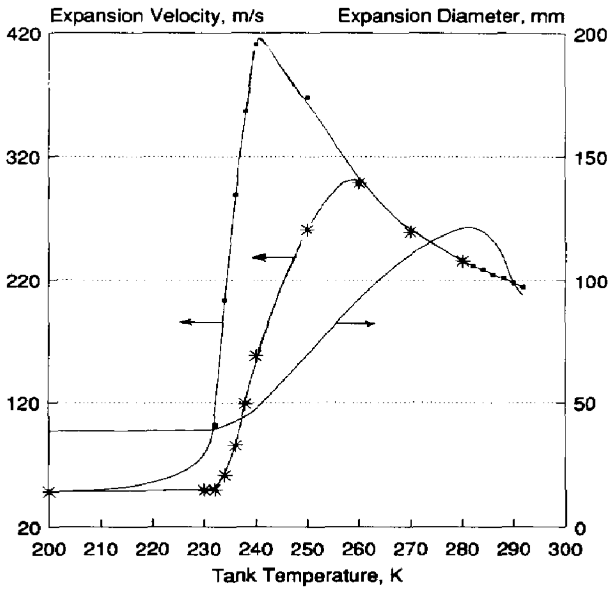

Fig. 3. Expansion velocity and diameter as a function of tank temperature. (■) Equilibrium velocity, (*) nonequilibrium velocity, and (—) expansion diameter. (propane, 1 m head, 50 mm hole.)

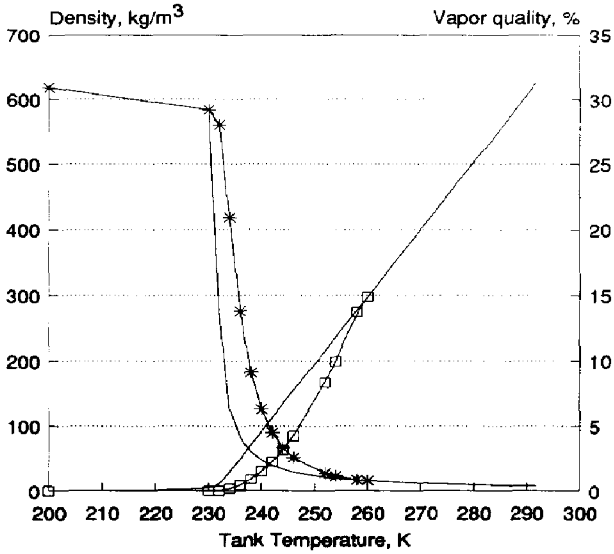

Fig. 4. Expansion zone model for propane gas, 1 m head, 50 mm orifice with constant pressure discharge. Equilibrium values are indicated by solid lines, nonequilibrium values by the symboled lines.

For the new model, further increases in temperature move G^*_{amb} farther down the curve from G^*_2, so the expansion zone diameter increases, which tends to decrease the expansion zone velocity. For temperatures above about 270 K, the vapor pressure curve increases rapidly, so $1-\eta_s$ which equals $1-\eta_c$ in eq. (21a) decreases rapidly with temperature. The consequent decrease in G^*_2 with temperature is partly compensated by an increase in the discharge coefficient, C_D, also shown in Fig. 5. The rapid decrease in G^*_2 for temperatures above about 270 K causes the expansion zone diameter to peak and then decrease (see Fig. 3 and 4). Flashing at or before the choke point occurs for temperatures above about 289 K in this case.

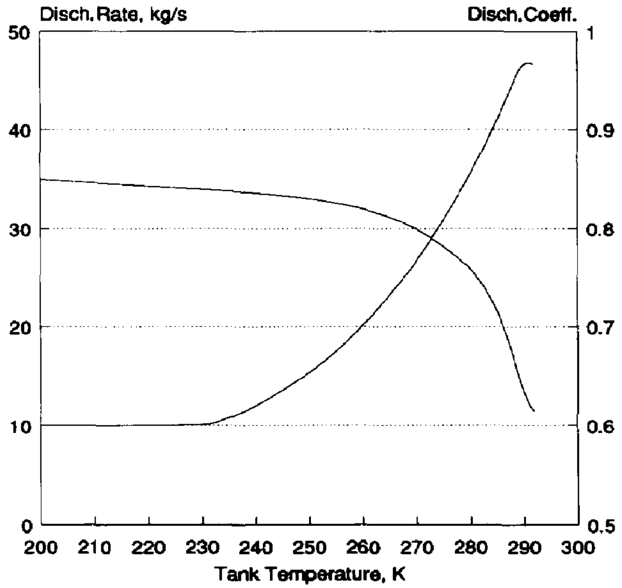

Fig. 5. Discharge rate predictions for constant pressure discharge (propane, 1 m head. 50 mm hole).

6.1 Estimation of shock wave

The error in ignoring shock wave effects can be estimated, using the following formulas for the pressure, density, and temperature ratio across a shock wave given by Nettleton [20]

$$\frac{P'_3}{P_2}=\frac{2\gamma M_S^2-(\gamma-1)}{\gamma+1} \tag{22a}$$

$$\frac{\rho'_3}{\rho_2}=\frac{(\gamma+1)M_S^2}{(\gamma-1)M_S^2+2} \tag{22b}$$

$$\frac{T'_3}{T_2}=\frac{\left[\gamma M_S^2-\frac{(\gamma-1)}{2}\right]\left[\frac{(\gamma-1)}{2}M_S^2+1\right]}{\left(\frac{\gamma+1}{2}\right)M_S^2} \tag{22c}$$

where $M_S=u_3/a$ is the Mach number, and $a^2=\gamma RT_s/M_C$ the sonic speed.

Figure 7 plots the pressure and temperature ratios given by eqs. (22a) and (22c) against tank temperature. The largest temperature ratio is 1.15, so the error in ignoring this temperature change is at most 15%. The presence of a shock wave produces a discontinuous decrease in pressure of

$$P'_3=\max\begin{cases}P_2/(P'_3/P_2)\\ P_a\end{cases}$$

which shortens the length of the expansion zone, but does not, per se, invalidate the assumptions inherent in applying eqs. (11)–(15).

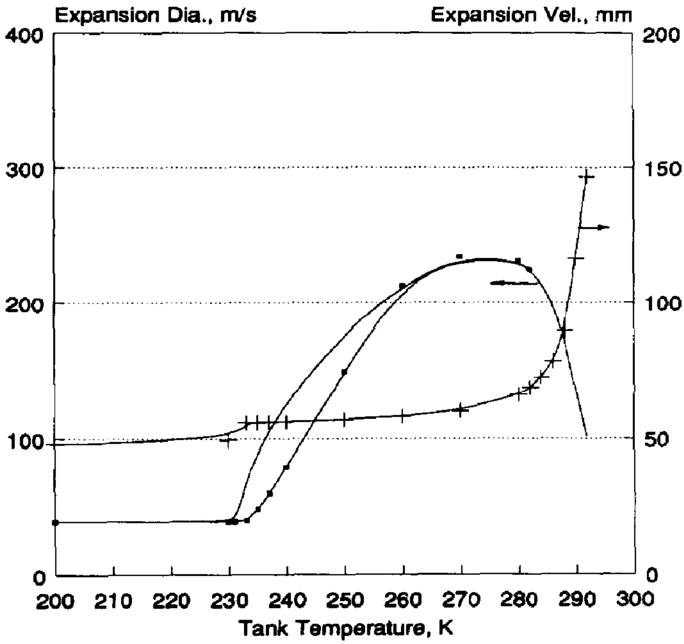

Fig. 6. Conventional expansion zone model for constant pressure discharge (propane, 1 m head, 50 mm hole). (■) Nonequilibrium expansion diameter, (—) equilibrium expansion diameter, and (+) expansion velocity.

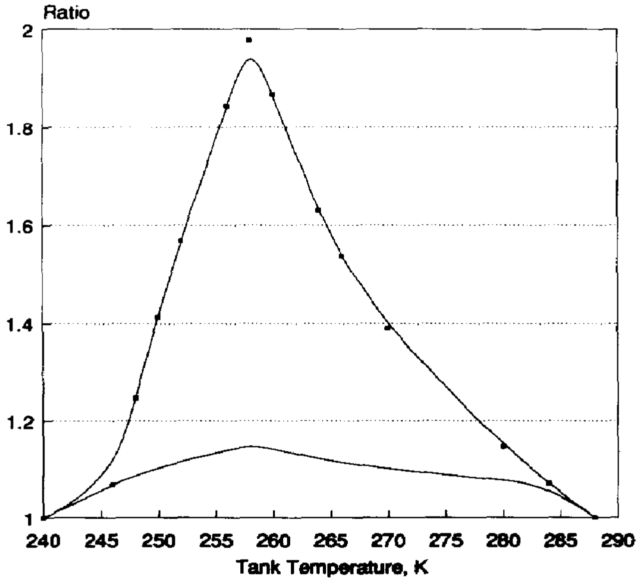

Fig. 7. Temperature and pressure change across shock wave. (■) P_3'/P_2, and (—) T_3'/T_2 (propane, 1 m head, 50 mm hole).

7. Conclusions

Two alternative models for the expansion zone velocity and diameter give predictions which agree for subcooled liquids, but differ substantially for gases and flashing liquids. For flashing liquids, both models are sensitive to the two-phase specific volume, v_3. Area, A_3, is linear in v_3 for the conventional model, wheras velocity, u_3, is linear in v_3 for the new model. Both model predictions seem more reasonable when the assumption is made that the equilibrium vapor quality, x_{3e}, is achieved only at high degrees of superheat. Experimental data are needed to decide which model is more nearly correct. Fortunately, though, the influence of the expansion zone model predictions upon subsequent dispersion modeling is usually absorbed in tuning the dispersion model. If the expansion zone model is changed, the jet dispersion model tuning should be checked and adjusted as needed.

8. Nomenclature

a	speed of sound, m s^{-1}
C_D	discharge coefficient, (–)
C_p	heat capacity at constant pressure, J kg^{-1} K^{-1}
C_v	heat capacity at constant volume, J kg^{-1} K^{-1}
G	mass flux, kg m^{-2} s^{-1}
G^*	$G/(P_0\rho_0)^{1/2}$, dimensionless mass flux
H_{GL}	heat of vaporization, $(H_G - H_L)$ sat, J kg^{-1}
k	value equal to or below C_p/C_v
M_s	Mach number of expansion zone velocity
P	pressure, Pa
S	entropy, J kg^{-1} K^{-1}
S_{GL}	$S_G - S_L$, J kg^{-1} K^{-1}
T	temperature, K
u	velocity, m s^{-1}
v	specific gravity, m^3 kg^{-1}
v_{GL}	$v_G - v_L$
w	mass discharge rate, kg s^{-1}
x	vapor quality, kg vapor/kg mixture
Greek	
ρ	density, kg/m^3
η	P/P_0
ω	parameter defined by eq. (7)

Subscripts

a	ambient
c	choke point, "critical" flow or Plane 2
G	vapor

L	liquid
0	stagnation conditions
s	saturation
0, 1, 2, 3	planes defined by Fig. 1

References

1 K. Moody and B.C.R. Ewan, Jets discharging to atmosphere, J. Loss Prev. Process Ind., 3 (1990) 68–76.
2 G.D. Kleinstein, Mixing in turbulent axially symmetric free jets, J. Spacecraft, 1(4) (1964) 403–408.
3 S.L. Bragg, Effect of compressibility on the discharge coefficient of orifices and convergent nozzles, J. Mech. Eng. Sci. 2 (1960) 35–44.
4 S.W. Churchill, Compressible flows, In: N.P. Cheremisinoff and R. Gupta (Eds.), Handbook of Fluids in Motion, Ann Arbor Science, Ann Arbor, MI, 1983, Chapter 8.
5 H.K. Fauske and M. Epstein, Source term considerations in connection with chemical accidents and vapour cloud modelling, J. Loss Prev. Process Ind., 1 (1988) 75–83.
6 H.L. Dryden, F.D. Murnaghan and H. Bateman, In: Hydrodynamics, Dover Publications, New York, 1936, p. 540.
7 R.E. Balzhiser and M.R. Samuels, Engineering Thermodynamics, Prentice Hall, Englewood Cliffs, NJ, 1977.
8 S.W. Churchill, The Practical Use of Theory in Fluid Flow, Book I, Inertial Flows, Etaner Press, Thornton, PA, 1980.
9 R.E. Henry, The two-phase critical discharge of initially saturated or subcooled liquid, Nuclear Sci. Eng., 41 (1970) 336–342.
10 S.D. Morris, Choking conditions for flashing one-component flows in nozzles and valves — A simple estimation method, I. Chem. E. Symp. Series No. 110, 1988, pp. 281–299.
11 F. Hardekopf and D. Mewes, The pressure ratio of critical two-phase flows, Chem. Eng. Technol., 12 (1989) 89–96.
12 H.K. Fauske, The Discharge of Saturated Water Through Tubes, Chem. Eng. Prog. Symp. Series, 61 (1965) 210–216.
13 R.E. Henry and H.K. Fauske, The two-phase critical flow of one-component mixtures in nozzles, orifices, and short tubes, Trans. Am. Soc. Mech. Eng. J. Heat Transfer, 93(5) (1971) 179–187.
14 J.C. Leung, A generalized correlation for one-component homogeneous equilibrium flashing choked flow, AIChE J., 32(10) (1986) 1743–1746.
15 J.C. Leung and M.A. Grolmes, A generalized correlation for flashing choked flow of initially subcooled liquid, AIChE J., 34(4) (1988) 688–691.
16 Design Institute of Emergency Relief Systems (DIERS) Report, Emergency Relief Systems for Runaway Chemical Reactions and Storage Vessels: A Summary of Multi-Phase Flow Methods, AIChE Pub. 132, FAI/83-27, October, 1983.
17 J.E. Huff, Multi-phase flashing flow in pressure relief systems, Plant/Operations Prog., 4(4) (1985) 191–199.
18 H.G. Fisher, An overview of emergency relief system design practice, Plant/Operations Prog., 10(1) (1991) 1–12.
19 S.M. Sami and T. Duong, A transient model for predicting nonhomogeneous non-equilibrium, critical, two-phase flows, Nuclear Technol. 83 (1989) 98–108.
20 M.A. Nettleton, Gaseous Detonations, Chapman and Hall, New York, 1987, p. 21.